Maximally entangled coherent states and strong violations of Bell-type inequalities

Christopher C. Gerry, Jihane Mimih, and Adil Benmoussa
Department of Physics and Astronomy, Lehman College, The City University of New York, Bronx, New York 10468-1589, USA
(Received 5 May 2009; published 17 August 2009)

Recently, Wildfeuer *et al.* [Phys. Rev. A **76**, 052101 (2007)] studied possible experiments demonstrating nonlocal correlation effects through the violation of various Bell-type inequalities by maximally path-entangled number states of the form $(|N\rangle|0\rangle + e^{i\varphi}|0\rangle|N\rangle)/\sqrt{2}$, the so-called *N*00*N* states, and some strong violations were found. In this paper, we re-examine the same Bell-type inequalities with respect to maximally path-entangled coherent states of the form $\mathcal{N}(|\alpha\rangle_a|0\rangle_b + e^{i\Phi}|0\rangle_a|\alpha\, e^{i\theta}\rangle_b)$. We find in many cases even stronger violations of the Bell-type inequalities than appear to be possible with the *N*00*N* states.

DOI: 10.1103/PhysRevA.80.022111 PACS number(s): 03.65.Ud, 42.50.Xa, 03.65.Wj, 03.67.Mn

I. INTRODUCTION

As is well known by now, no local realistic theory is capable of making predictions that are in complete agreement with those of standard quantum mechanics whenever entangled states are involved as was shown by Bell [1] for a spin-singlet state for two particles, a bipartite entangled state. The spin-singlet state is, in fact, an example of a maximally entangled state, and Bell showed that such a state would, according to quantum mechanics, give rise to nonlocal effects as exhibited by the statistical violations of a certain inequality. Observations of such violations falsify all hidden-variable theories featuring local realism. A particularly interesting example of a bipartite maximally entangled state of many particles consists of a superposition of the extremal states where all the particles in one mode or the other. In a collection of two-level atoms, the extremal states are those with all atoms in their excited states and those with all atoms in their ground states. Superpositions of such states are known to be useful for the purpose of obtaining quantum-enhanced frequency standards and for improved accuracy of atomic clocks [2]. In the realm of optics, there has recently been much interest in the use of two-mode maximally entangled number states, sometimes called *N*00*N* states, given by

$$|\Psi_N\rangle = \frac{1}{\sqrt{2}}(|N\rangle_a|0\rangle_b + e^{i\varphi}|0\rangle_a|N\rangle_b), \tag{1}$$

where *a* and *b* represent two spatially separated modes, for applications in quantum metrology and quantum sensing [3] at the Heisenberg limit and for quantum interferometric photolithography beyond the Rayleigh diffraction limit [4]. In the case of Heisenberg-limited interferometry, the uncertainty in the measurements of phase shifts is given by $\Delta\phi_{\mathrm{HL}}=1/N$, an improvement by a factor of $1/\sqrt{N}$ over the standard quantum limit $\Delta\phi_{\mathrm{SQL}}=1/\sqrt{N}$. Quite recently, Wildfeuer *et al.* [5] studied possible nonlocal correlation experiments that could be performed with the states of Eq. (1) for the specific choice of relative phase $\varphi=\pi$ and showed that violations of a Clauser-Horne (CH) [6] form of Bell's inequality [7], and various other Bell-type inequalities, especially those obtained by Janssens *et al.* [8], can be strong. In some cases, the violation is independent of the total number of photons *N*, while in others, such as the Clauser-Horne inequality, the violation does depend on *N* but rapidly diminishes with increasing *N*. In fact, in the context of the Clauser, Horne, Shimony, and Holt (CHSH) [9] form of Bell's theorem, there have already been studies—theoretical and experimental [10]—for the special case of the *N*00*N* states for $N=1$. As far as we are aware, the work by Wildfeuer *et al.* [5] is the first theoretical discussion on violations of such inequalities for the *N*00*N* states for $N>1$.

In the present paper we re-examine the Bell-type inequalities studied in [5] but instead of *N*00*N* states we consider maximally entangled coherent states (MECSs) of the form

$$|\Psi_\alpha\rangle = \mathcal{N}(|\alpha\rangle_a|0\rangle_b + e^{i\Phi}|0\rangle_a|\alpha\, e^{i\theta}\rangle_b), \tag{2}$$

where the normalization factor is given by

$$\mathcal{N} = \frac{1}{\sqrt{2}}[1 + e^{-|\alpha|^2}\cos\varphi]^{-1/2}. \tag{3}$$

In the number state basis, the MECS is decomposed according to

$$|\Psi_\alpha\rangle = \mathcal{N}e^{-|\alpha|^2/2}\sum_{n=0}^{\infty}\frac{\alpha^n}{\sqrt{n!}}[|n\rangle_a|0\rangle_b + e^{i(n\theta+\Phi)}|0\rangle_a|n\rangle_b], \tag{4}$$

from which we see that MECSs are *superpositions* of *N*00*N* states. We are motivated to consider the nonlocality properties if MECS by the fact that elsewhere [11] we have shown these MECS can be used, in place of the *N*00*N* states, to perform Heisenberg-limited interferometry yielding phase-shift uncertainties which are Heisenberg limited in terms of the average number of photons in the coherent state, i.e., $\Delta\phi=1/\bar{n}$, where $\bar{n}=|\alpha|^2$. That is, in the context of interferometry they have the capacity to produce results that closely parallel those obtained by from *N*00*N* states and, thus, it seemed worthwhile to study the possible use of these states for tests of quantum mechanics versus local realistic theories. Furthermore, they may have the advantage of being easier to produce than the *N*00*N* states as one does not first have to generate number states, a daunting proposition for the necessary states of high *N*, whereas coherent states of more or less arbitrary amplitude are available from phase-stabilized lasers. However, the generation of the MECS and the *N*00*N* states from an initial coherent state $|\alpha\rangle$ or number state $|N\rangle$, respectively, generally requires large cross-Kerr nonlineari-

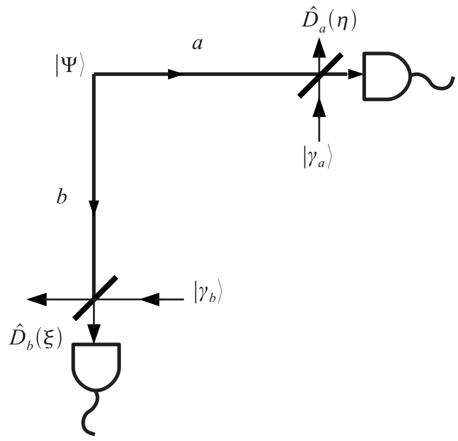

FIG. 1. Unbalanced homodyne detection scheme for a Bell-type experiment with MECS of Eq. (2).

ties [12], or large self-Kerr interactions [13], a challenge due to the nonavailability of the required large third order nonlinear susceptibilities, though there is some hope that large cross-Kerr interactions may eventually become available through the techniques of electromagnetically induced transparency [14]. One first should generate a single-mode coherent superposition state $|\zeta\rangle+e^{i\vartheta}|-\zeta\rangle$, for example, and then mix it with the coherent state $|-i\zeta\rangle$ on a 50:50 beam splitter to generate the MECS, in this case, the MECS $|\sqrt{2}\zeta\rangle|0\rangle+e^{i\vartheta}|0\rangle|-\sqrt{2}\zeta\rangle$. There was a recent work by Lee [15] on the prospect of using linear optics to implement measurement-induced large cross-Kerr nonlinearities along the lines first discussed by Knill *et al.* [16]. Another possibility is to use weak cross-Kerr nonlinearities and large amplitude coherent states to generate the MECS based on a proposal by Gerry [17] and as modified by Jeong [18(a)] and, more recently, by He *et al.* [18(b)]. Recently, Glancy and de Vasconcelos [19] reviewed various methods that have been proposed for generating the optical coherent-state superpositions. For the purposes of this paper, we shall just assume the availability of MECS in the form of Eq. (2).

In demonstrating nonlocal correlations of entangled coherent states, we shall follow Ref. [5] in using their proposed measurement schemes to examine the same forms of Bell's theorem as they studied, namely, the form given by CH [6], that of CHSH [7], and forms discussed by Janssens *et al.* [9]. The measurements are assumed to be performed with the unbalanced homodyne detection scheme of Banaszek and Wódkiewicz [10] in which the required correlation functions are obtained through the operational definitions of the two-mode Q function and the two-mode Wigner function. A sketch of the proposed experimental scheme is given in Fig. 1. The spatially separated beams labeled a and b of the prepared entangled state $|\Psi\rangle$ are directed toward beam splitters operating in the limit of transmissivity $T\to 1$ (for unbalanced homodyning), which have strong coherent fields (the local fields) in their other input ports, i.e., states of the form $|\gamma\rangle$ where $|\gamma|\to\infty$. Under these conditions, the beam splitters act as displacement operators on the a and b input beams where the displacement operator has the form $\hat{D}(\gamma\sqrt{1-T})$, where $\hat{D}(\lambda)=\exp(\lambda\hat{a}^{\dagger}-\lambda^{*}\hat{a})$ [20] and where $\lambda=\gamma\sqrt{1-T}$, such that the displacement operators for the a and b beams are $\hat{D}_a(\mu)$ and $\hat{D}_b(\nu)$, respectively, where $\mu=\gamma_a\sqrt{1-T}$ and $\nu=\gamma_b\sqrt{1-T}$. The parameters μ and ν will play the roles of the angle settings of the Stern-Gerlach magnets in experiments with entangled spins states, such as the spin-singlet state $(|\uparrow\rangle_a|\downarrow\rangle_b-|\downarrow\rangle_a|\uparrow\rangle_b)/\sqrt{2}$, or of the polarizer settings for an experiment performed with two-photon polarization entangled states of the form $(|H\rangle_a|V\rangle_b-|V\rangle_a|H\rangle_b)/\sqrt{2}$. That is, the correlation functions we shall obtain will depend on the complex parameters μ and ν. These parameter settings can be adjusted by changing the strengths of the strong coherent-state field amplitudes and phases in order to facilitate the measurements required to obtain the quantum-mechanical averages of the correlation functions. Overall, for the MECS we find greater degree of violation of the various Bell-type inequalities considered than is possible for the $N00N$ states.

The paper is organized as follows. In Sec. II, we consider the on-off detection scheme, which leads to the CH form of Bell's theorem, while in Sec. III we consider the CHSH form of Bell's theorem using displaced parity operators. In Sec. IV we study the various Bell-type inequalities given by Janssens *et al.* [8], and Sec. V contains some brief remarks. Lastly, for the purpose of comparison to the results of the present paper, in the Appendix we summarize some of the $N00N$ state results of Ref. [5] and extend them to the case for $\varphi=0$. In redoing the calculations of Ref. [5], we found a couple of discrepancies with the results in that paper. These are minor and do not change the conclusions of that work. We also include some useful $N00N$ state results that were not presented graphically in Ref. [5], namely, the $N00N$ state results for the CHSH form of Bell's inequality. Again, this is for the purpose of comparison with our MECS results.

II. BELL EXPERIMENT WITH A DISPLACED ON-OFF DETECTION SCHEME

As in Ref. [5], we begin with the homodyne detection scheme depicted in Fig. 1. Each beam is to be subjected to homodyne detection performed using a strong local oscillator on a beam splitter as described above. On-off photon detection is described by the positive operator valued measure (POVM),

$$\hat{\Pi}_0=|0\rangle\langle 0|,\quad \hat{\Pi}_1=\hat{\mathbf{I}}-|0\rangle\langle 0|=\sum_{k=1}^{\infty}|k\rangle\langle k|. \tag{5}$$

The POVM for the homodyne on-off measurement, which explicitly takes into account the displacement operator that occurs just before the photon detector is given by the operators,

$$\hat{Q}(\mu)=\hat{D}(\mu)\hat{\Pi}_0\hat{D}^{\dagger}(\mu)=|\mu\rangle\langle\mu|, \tag{6}$$

$$\hat{P}(\mu)=\hat{D}(\mu)\hat{\Pi}_1\hat{D}^{\dagger}(\mu), \tag{7}$$

where $\hat{Q}(\mu)+\hat{P}(\mu)=\hat{\mathbf{I}}$, and where μ is a complex number and $|\mu\rangle$ is a coherent state. The photon detectors pictured in Fig. 1 are assumed to be lossless. The expectation value of the operator $\hat{Q}(\mu)$ is just the Q function phase-space quasiprobability distribution. The expectation value $Q(\mu) = \langle \hat{Q}(\mu) \rangle$ represents the probability of detecting no photons after the displacement of the beam by the amount μ as determined by the amplitude and phase of the strong local coherent field. This corresponds to an "off" detection. The expectation value $\langle \hat{P}(\mu) \rangle$ represents the probability of detecting one or more photons in the displaced beam but is otherwise insensitive to the actual number of photons detected. This corresponds to an "on" detection. We obtain a binary result by assigning a "1" to a detector click and a "0" otherwise. The operators corresponding to a correlated measurement of the displaced vacua of modes a and b is given by $\hat{Q}_a(\mu) \otimes \hat{Q}_b(\nu)$, which have the expectation value

$$Q_{a,b}(\mu,\nu) = \langle \Psi_\alpha | \hat{Q}_a(\mu) \otimes \hat{Q}_b(\nu) | \Psi_\alpha \rangle = |{}_a\langle \mu | {}_b\langle \nu | \Psi_\alpha \rangle|^2. \tag{8}$$

The probabilities for individual measurements on modes a and b are given by

$$Q_a(\mu) = \langle \Psi_\alpha | \hat{Q}_a(\mu) \otimes \hat{\mathbf{I}}_{\mathbf{b}} | \Psi_\alpha \rangle, \tag{9}$$

$$Q_b(\nu) = \langle \Psi_\alpha | \hat{\mathbf{I}}_{\mathbf{a}} \otimes \hat{Q}_b(\nu) | \Psi_\alpha \rangle. \tag{10}$$

We find that

$$Q_{ab}(\mu,\nu) = |\mathcal{N}|^2 \exp[-(|\mu|^2 + |\nu|^2 + |\alpha|^2)] |\exp(\mu^* \alpha) + e^{i\varphi} \exp(\nu^* \alpha\, e^{i\theta})|^2, \tag{11}$$

$$Q_a(\mu) = |\mathcal{N}|^2 e^{-|\mu|^2} \{1 + e^{-|\alpha|^2 + \mu\alpha^* + \mu^*\alpha} + 2\,\mathrm{Re}[e^{i\varphi} e^{-|\alpha|^2 + \mu\alpha^*}]\}, \tag{12}$$

$$Q_b(\nu) = |\mathcal{N}|^2 e^{-|\nu|^2} \{1 + e^{-|\alpha|^2 + \nu\alpha^* e^{-i\theta} + \nu^*\alpha e^{i\theta}} + 2\,\mathrm{Re}[e^{i\varphi} e^{-|\alpha|^2 + \nu^*\alpha e^{i\theta}}]\}. \tag{13}$$

From the completeness relation $\hat{Q}(\mu) + \hat{P}(\mu) = \hat{\mathbf{I}}$, we can obtain the probabilities for the correlated and single detector counts in terms of the Q functions according to

$$P_a(\mu) = 1 - Q_a(\mu), \tag{14}$$

$$P_b(\nu) = 1 - Q_b(\nu), \tag{15}$$

$$P_{ab}(\mu,\nu) = 1 - Q_a(\mu) - Q_b(\nu) + Q_{ab}(\mu,\nu). \tag{16}$$

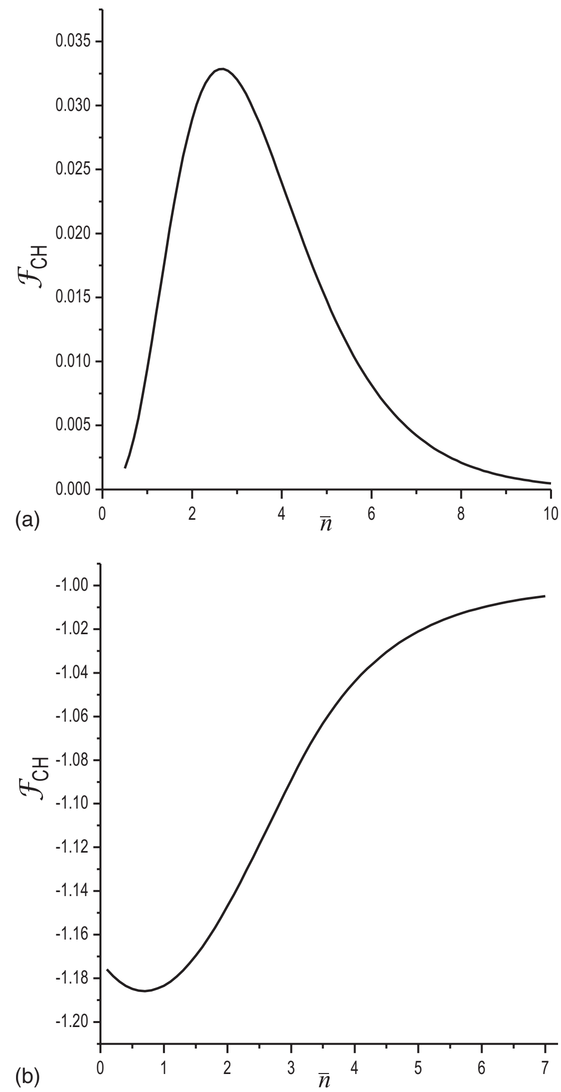

FIG. 2. The CH quantity versus the average photon number $\bar{n}$ for (a) $\Phi = 0$ and (b) $\Phi = \pi$. The former results are obtained via maximization (there are no violations for the minimum in this case), whereas the latter is obtained via minimization.

From these, one can construct the Clauser-Horne function [6],

$$\mathcal{F}_{\mathrm{CH}} = P_{ab}(\mu,\nu) - P_{ab}(\mu,\nu') + P_{ab}(\mu',\nu) + P_{ab}(\mu',\nu') - P_a(\mu') - P_b(\nu), \tag{17}$$

which, for a local hidden-variable theory, satisfies the inequality $-1 \le \mathcal{F}_{\mathrm{CH}} \le 0$.

Our results for the numerical maximization or minimization of $\mathcal{F}_{\mathrm{CH}}$ obtained with the MECS, which are shown in Fig. 2, where we plot $\mathcal{F}_{\mathrm{CH}}$ versus $\bar{n} = |\alpha|^2$. For the case $\Phi = 0$, we find violations of the inequality only via maximization, for $\mathcal{F}_{\mathrm{CH}} > 0$, and these violations are small. For $\Phi = \pi$, we find much stronger violations of the inequality but this time in the regime $\mathcal{F}_{\mathrm{CH}} < -1$. In both cases, the violations are for average photon numbers in the range $0 < \bar{n} < 6$. In both

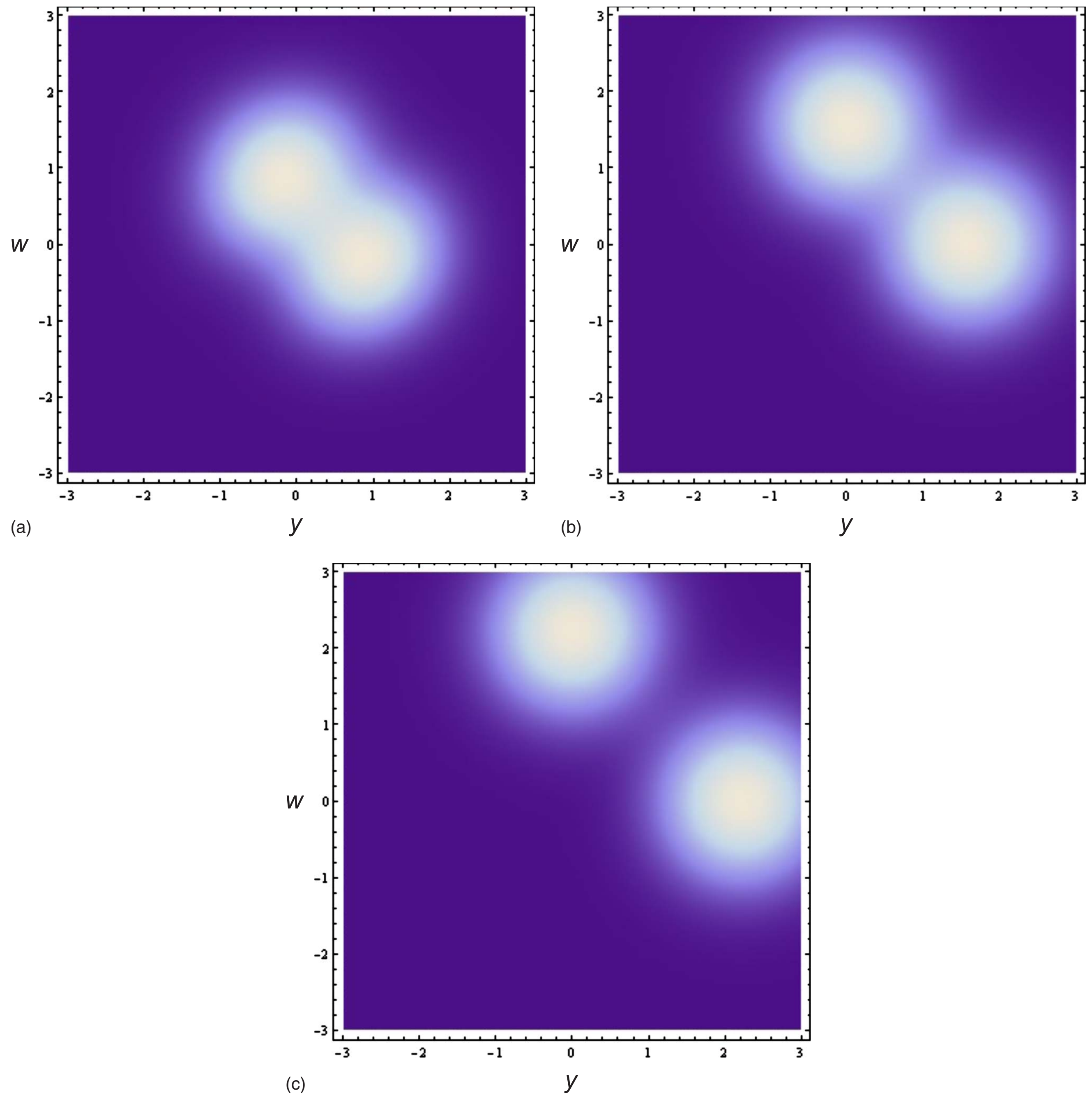

FIG. 3. (Color online) Density plots of the marginal Q function $Q_m(y,w)$ for (a) $\bar{n}=1$, (b) $\bar{n}=5$, and (c) $\bar{n}=10$.

cases, $\mathcal{F}_{\rm CH}$ goes to the respective boundaries, for the former and -1 for the latter as $\bar{n}$ goes to 0 and as it becomes very large. We find no dependence on the angle θ. The $N00N$ states for both $\varphi=0$, π yield identical results for $\mathcal{F}_{\rm CH}$ and strong violations of the inequality are obtained only for $N=1$ as can be seen in Fig. 10. In contrast, the violations of the inequality obtained with the MECS occur over a somewhat wider range of average photon numbers.

Following [5], we examine the corresponding marginal distributions of the function $Q_{ab}(\mu,\nu)$. Setting $\mu=x+iy$, $\nu=u+iw$, where x, y, u, and w are real variables, the marginal distribution is given by

$$\begin{aligned} Q_m(y,w) &= \int_{-\infty}^{\infty}\int_{-\infty}^{\infty} Q_{ab}(x,y,u,w)dxdu, \\ &= |\mathcal{N}|^2\pi e^{-y^2-w^2-|\alpha|^2}\{e^{\mathrm{Re}(\alpha^2)}e^{2y\,\mathrm{Im}(\alpha)} \\ &\quad + e^{\mathrm{Re}(\alpha^2e^{2i\theta})}e^{2w\,\mathrm{Im}(\alpha e^{i\theta})} \\ &\quad + 2\,\mathrm{Re}[e^{i\theta}e^{(\alpha^{*2}+\alpha^2e^{2i\theta})/4}e^{i(y\alpha^*-w\alpha e^{i\theta})}]\}. \end{aligned} \quad (18)$$

In Fig. 3 we have plotted the marginal distributions for the cases, where $\Phi=\pi$ and $\alpha=\sqrt{\bar{n}}e^{i\pi/4}$ and for the choices $\bar{n}=1$, 5, and 10. We see that the distribution consists of two peaks located in the y-w plane on opposite sides for the line $y=w$ for all values of $\bar{n}$, though the peaks become more separated for increasing $\bar{n}$. In contrasts, the corresponding distributions for the $N00N$ states have this double peak form only for the case $N=1$, the case for which the CH inequality is most strongly violated; whereas for $N>1$, there are additional peaks such that the distribution becomes more symmetric and the violations of the inequality are quite small. These more symmetric distributions seem to be correlated with reduced violations of the CH inequality for $N>1$. The interesting point is that the distributions for the MECS for different $\bar{n}$ are like that of the $N00N$ for $N=1$, and this may be reflected in the fact that violations for the CH inequality are large over a fairly wide range of $\bar{n}$.

We also calculate the linear correlation coefficient $r=\text{cov}(y,w)/(\Delta y \Delta w)$, where

$$\text{cov}(y,w) = \int_{-\infty}^{\infty}\int_{-\infty}^{\infty}(y-\bar{y})(w-\bar{w})Q_m(y,w)dydw, \quad (19)$$

which yields $r=-0.3$, -0.55, and -0.71, respectively, for the above choices of average photon number. The correlations according to this measure, actually anticorrelations, appear to increase with increasing $\bar{n}$ even though the violations of the CH inequality decrease. This suggests that linear correlations are not the whole story in connection with the violations of the CH inequality. On the other hand, as we show in the next section, increasing correlations (anticorrelations) do seem to be strongly connected with the increasing violation with $\bar{n}$ of another form of Bell's theorem, that of Clauser, Horne, Shimony, and Holt [7].

III. PARITY MEASUREMENTS AND THE CLAUSER, HORNE, SHIMONY, AND HOLT INEQUALITY

The parity operator of a single-mode quantized field is

$$\hat{\Pi}(0) = \exp(i\hat{n}\pi) = \sum_{k=0}^{\infty}|2k\rangle\langle 2k| - \sum_{k=0}^{\infty}|2k+1\rangle\langle 2k+1|. \quad (20)$$

The POVM for our measurements is given as the displaced parity operator

$$\hat{\Pi}(\mu) = \hat{D}(\mu)\hat{\Pi}(0)\hat{D}^{\dagger}(\mu), \quad (21)$$

which, up to a factor of $2/\pi$, is the Wigner operator $\hat{W}(\mu)=(2/\pi)\hat{\Pi}(\mu)$, whose expectation value is just the Wigner function $W(\mu)=\langle\hat{W}(\mu)\rangle$. For the two-mode case, we have

$$\hat{\Pi}_{ab}(\mu,\nu) = [\hat{D}_a(\mu)\hat{\Pi}_a(0)\hat{D}_a^{\dagger}(\mu)] \otimes [\hat{D}_b(\nu)\hat{\Pi}_b(0)\hat{D}_b^{\dagger}(\nu)]. \quad (22)$$

The corresponding Wigner operator is $\hat{W}_{ab}(\mu,\nu)=(4/\pi^2)\hat{\Pi}_{ab}(\mu,\nu)$. Setting $\Pi_{ab}(\mu,\nu)=\langle\Psi_\alpha|\hat{\Pi}(\mu,\nu)|\Psi_\alpha\rangle$, we can construct the CHSH inequality [7] as $-2\leq\mathcal{B}\leq 2$, where

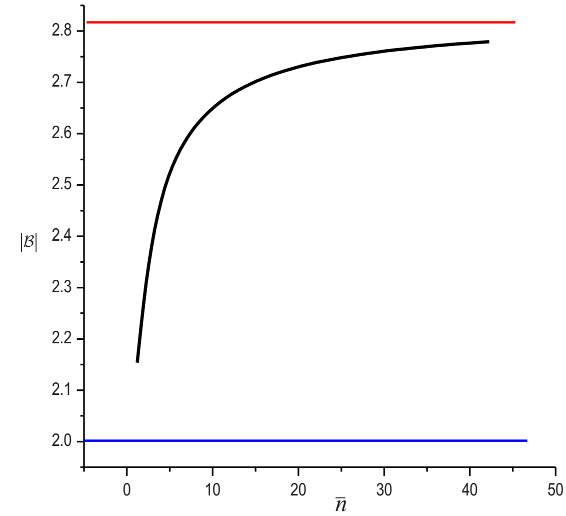

FIG. 4. (Color online) A plot of the CHSH quantity $|\mathcal{B}|$ versus $\bar{n}$. The CHSH inequality is violated for $2<|\mathcal{B}|\leq 2\sqrt{2}$; the boundaries are given by the upper and lower horizontal lines.

$$\mathcal{B} = \hat{\Pi}_{ab}(\mu,\nu) + \hat{\Pi}_{ab}(\mu',\nu) + \hat{\Pi}_{ab}(\mu,\nu') - \Pi_{ab}(\mu',\nu'), \quad (23)$$

and where

$$\hat{\Pi}_{ab}(\mu,\nu) = |\mathcal{N}|^2[e^{-2|\nu|^2-2|\nu-\alpha|^2} + e^{-2|\nu-\alpha e^{i\theta}|^2-2|\mu|^2} + 2\,\text{Re}(e^{i\Phi}e^{-|\alpha|^2}e^{-2|\mu|^2+2\mu\alpha^*}e^{-2|\nu|^2+2\nu^*\alpha e^{i\theta}})]. \quad (24)$$

We numerically search for the extrema of $\mathcal{B}$ for the cases $\Phi=0$, π, and find—apart from sign—identical results for a given $\bar{n}$ (though the parameters that achieve these extrema may be different). For $\Phi=0$ $\mathcal{B}$ is positive and for $\Phi=\pi$ it is negative. We again find no dependence of the angle θ. In Fig. 4 we plot $|\mathcal{B}|$ against $\bar{n}$ and we see that the CHSH inequality is violated for the entire range of $\bar{n}$, and for increasing larger values asymptotically approaches the so-called Tsirelson bound [21]: the maximally allowed value of the CHSH function $|\mathcal{B}|_{\max}=2\sqrt{2}$. This behavior is in sharp contrast to what happens for the $N00N$ states, which violates the CHSH inequality only for the case $N=1$ (see the Appendix), the case studied some years ago by Banaszek and Wódkiewicz [10].

We next examine the marginal Wigner function defined as

$$W_m(y,w) = \int_{-\infty}^{\infty}\int_{-\infty}^{\infty}W_{ab}(x,y,u,w)dxdu,$$
$$= \frac{2}{\pi}|\mathcal{N}|^2\{e^{-2y^2-2w^2-2|\alpha|^2-2iy(\alpha-\alpha^*)+2\,\text{Re}(\alpha^2)} + e^{-2y^2-2w^2-2|\alpha|^2-2iw(\alpha e^{i\theta}-\alpha^* e^{-i\theta})+2\,\text{Re}(\alpha^2 e^{2i\theta})} + 2\,\text{Re}[e^{i\Phi}e^{-|\alpha|^2-2y^2+2iy\alpha^*-2w^2-2iw\alpha e^{i\theta}}e^{(\alpha^{*2}+\alpha^2 e^{2i\theta})/2}]\}, \quad (25)$$

where, as before we have set $\mu=x+iy$, $\nu=u+iw$. In Fig. 5 we picture this distribution for the case $\Phi=\pi$ and the same val-

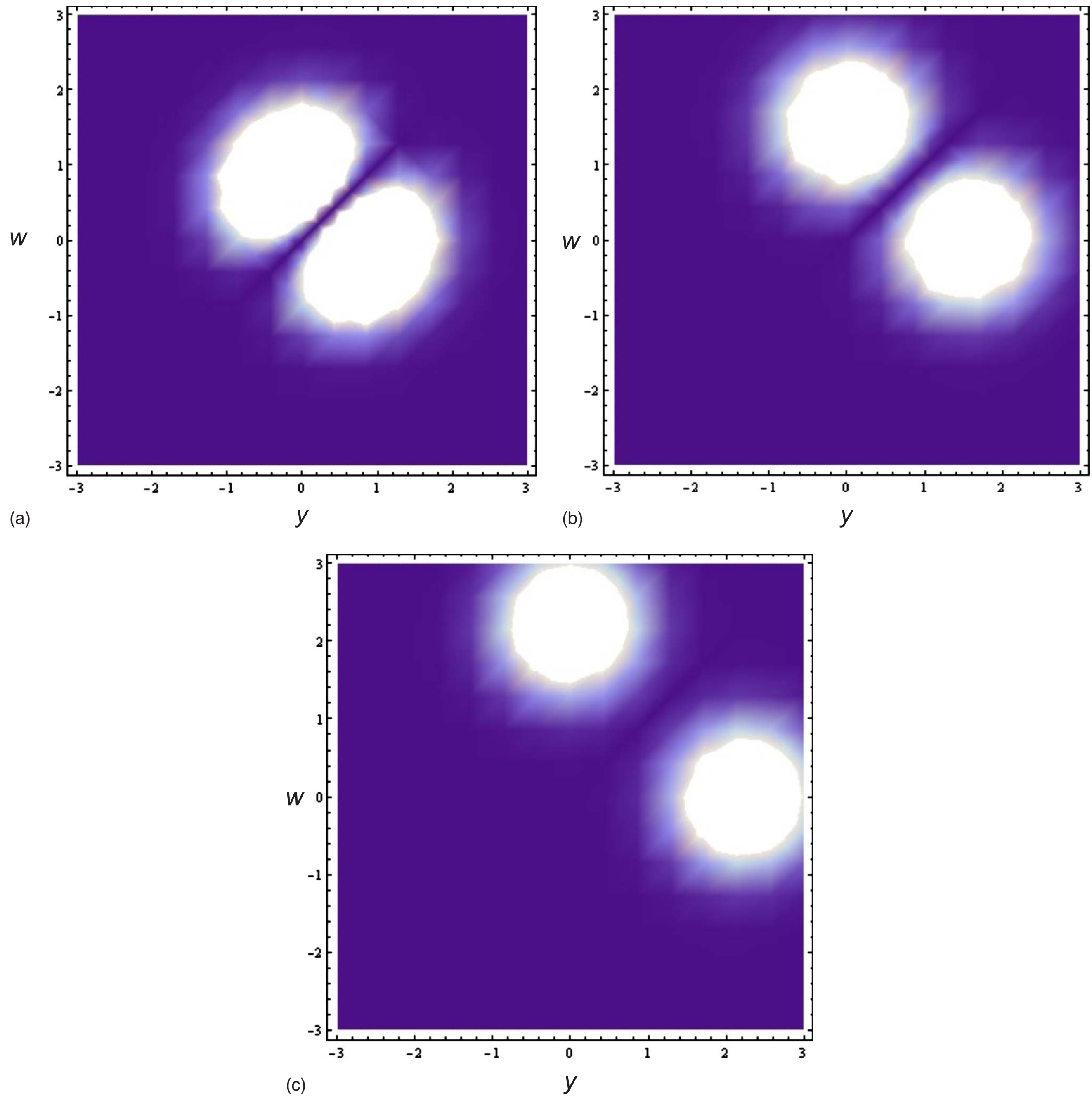

FIG. 5. (Color online) Density plots of the marginal Wigner function $W_m(y,w)$ for (a) $\bar{n}=1$, (b) $\bar{n}=5$, and (c) $\bar{n}=10$.

ues of $\bar{n}$ chosen above. Again we find sharp contrast with the results reported in Ref. [5] for the $N00N$ state. As in the case of the marginal Q function, we see two peaks located along the line $y=w$ for all values of $\bar{n}$, becoming increasingly separated for increasing $\bar{n}$. In contrast, the distribution for the $N00N$ states is similar to that of the corresponding marginal Q function, becoming more symmetric with increasing N (see Ref. [5]), resembling our results only for the case with $N=1$, that being the only $N00N$ state that violates the CHSH inequality. Given the increasing violation of the CHSH inequality with increasing $\bar{n}$, it appears that correlation between the shape of the marginal Wigner function and the violation of the inequality is much stronger than the correlation between the shape of the marginal Q function and the violation of the CH inequality, which diminishes for increasing $\bar{n}$. Finally, we used the marginal Wigner function to calculate the linear correlation coefficient and found $r=-0.5$, -0.71, and -0.83 for the above photon numbers, respectively.

IV. INEQUALITIES OF JANSSENS *ET. AL*

The CH Bell inequality is a specific form of an inequality involving four correlated events, where at most two are intersected at the same time. As pointed out in [5], Pitwosky [20] derived the set of all possible Bell-type inequalities for three or four correlated events, these being

$$0 \leq p_i - p_{ij} - p_{ik} + p_{jk}, \tag{26}$$

$$p_i + p_j + p_k - p_{ij} - p_{ik} - p_{jk} \leq 1, \tag{27}$$

$$-1 \leq p_{ik} - p_{jl} + p_{il} + p_{jk} - p_i - p_k \leq 0, \tag{28}$$

for i, j, k, and l all different. The last is just the CH inequality while the previous two are inequalities associated with the so-called Bell-Wigner polytope for three correlated events. For six correlated events, where two are intersected, Janssens *et al.* [8] constructed the inequalities,

$$p_i + p_j + p_k + p_l - p_{ij} - p_{ik} - p_{il} - p_{jk} - p_{jl} - p_{kl} \leq 1, \tag{29}$$

$$2p_i + 2p_j + 2p_k + 2p_l - p_{ij} - p_{ik} - p_{il} - p_{jk} - p_{jl} - p_{kl} \leq 3, \tag{30}$$

$$0 \leq p_i - p_{ij} - p_{ik} - p_{il} + p_{jk} + p_{jl} + p_{kl}, \tag{31}$$

$$p_i + p_j + p_k - 2p_l - p_{ij} - p_{ik} + p_{il} - p_{jk} + p_{jl} + p_{kl} \leq 1. \tag{32}$$

For the on-off detection scheme, the probabilities in Eqs. (29)–(32) are replaced by the probabilities of Eqs. (14)–(16) to obtain the functions

$$J_1 = Q(\alpha) + Q(\beta) + Q(\gamma) + Q(\delta) - Q(\alpha,\beta) - Q(\alpha,\gamma) - Q(\alpha,\delta) - Q(\beta,\gamma) - Q(\beta,\delta) - Q(\gamma,\delta), \tag{33}$$

$$J_2 = 2Q(\alpha) + 2Q(\beta) + 2Q(\gamma) + 2Q(\delta) - Q(\alpha,\beta) - Q(\alpha,\gamma) - Q(\alpha,\delta) - Q(\beta,\gamma) - Q(\beta,\delta) - Q(\gamma,\delta), \tag{34}$$

$$J_3 = Q(\alpha) - Q(\alpha,\beta) - Q(\alpha,\gamma) - Q(\alpha,\delta) + Q(\beta,\gamma) + Q(\beta,\delta) + Q(\gamma,\delta), \tag{35}$$

$$J_4 = Q(\alpha) + Q(\beta) + Q(\gamma) - 2Q(\delta) - Q(\alpha,\beta) - Q(\alpha,\gamma) + Q(\alpha,\delta) - Q(\beta,\gamma) + Q(\beta,\delta) + Q(\gamma,\delta), \tag{36}$$

where the correspondences between the indices in Eqs. (29) and (33) are $i \to \alpha$, $j \to \beta$, $k \to \gamma$, and $l \to \delta$. For local realistic theories, these functions satisfy the inequalities $J_1 \leq 1$, $J_2 \leq 3$, $0 \leq J_3$, and $J_4 \leq 1$.

In Figs. 6–9, we plot, respectively, the quantities J_1 to J_4 against $\bar{n}$. For some of them we find considerable differences as compared with the $N00N$ state results. For J_1, Wildfeuer *et al.* [5] found a constant violation of the corresponding inequality $J_1 \leq 1$ at the value $J_1 = 2$ independent of N and we found identical results for the cases $\varphi = 0$ and π (Fig. 12). For the MECS, we find that for $\Phi = 0$ there is a dependence on the angle θ, which we take to be 0 or π, and that for $\bar{n} \sim 1.5$, and for $\theta = 0$ a larger violation of the inequality is obtained than seems to be possible with the $N00N$ states. On the other hand, for $\Phi = \pi$ we find no dependence on θ and find a constant violation at the value $J_1 = 2$ except for small values of $\bar{n}$ for which $J_1 \to 1$.

For J_2, the $N00N$ states violate the corresponding inequality $J_2 \leq 3$ at the constant value $J_2 = 4$ independent of N and again identical results for $\varphi = 0$ and π (Fig. 12). For the MECS with $\Phi = 0$, we find a dependence on θ and results that asymptotically approach $J_2 = 4$ for large $\bar{n}$, as shown in Fig. 7(a). We note, though, a large violation of this inequality for the $\theta = 0$ case in the vicinity of $\bar{n} = 1$. For $\Phi = \pi$, the MECS maintain the value $J_2 = 4$ for all but the lowest $\bar{n}$, for which $J_2 \to 3$, and is independent of θ as given in Fig. 7(b). This behavior is quite similar to what we found for J_1.

With regard to J_3, the authors of Ref. [5] found relatively small violations of the Bell inequality $0 \leq J_3$, finding the greatest violation of $J_3 = -0.25$ for $N = 1$ (Fig. 14). For the MECS, as seen in Fig. 8 we find large violations of the inequality, where $J_3 \to -1$ asymptotically for all choices of θ and Φ.

Finally, for the inequality $J_4 \leq 1$, the $N00N$ states violation is at about $J_4 = 1.6$ as seen in Fig. 15 for all $N \geq 4$. For the MECS with $\Phi = 0$, we find much larger violations for both $\theta = 0$ and π, the former giving violations up to about

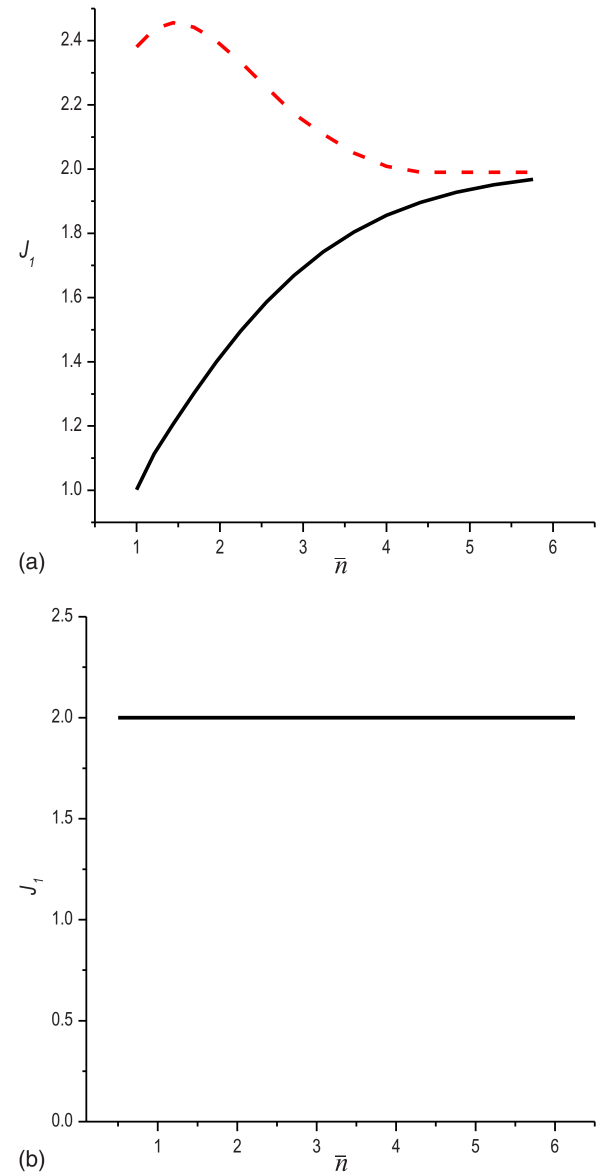

FIG. 6. (Color online) Extremal values of J_1 for (a) $\Phi = 0$ and (b) $\Phi = \pi$. The dashed line in (a), and in the remaining figures, is for $\theta = 0$ and the solid line is for $\theta = \pi$.

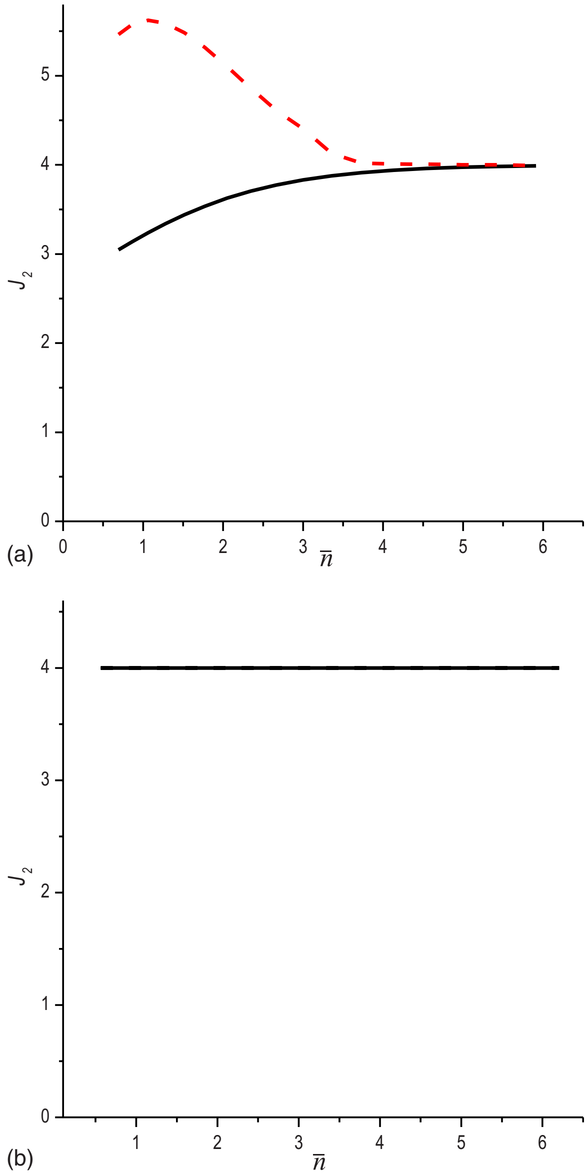

FIG. 7. (Color online) Extremal values of J_2 for (a) $\Phi=0$ and (b) $\Phi=\pi$.

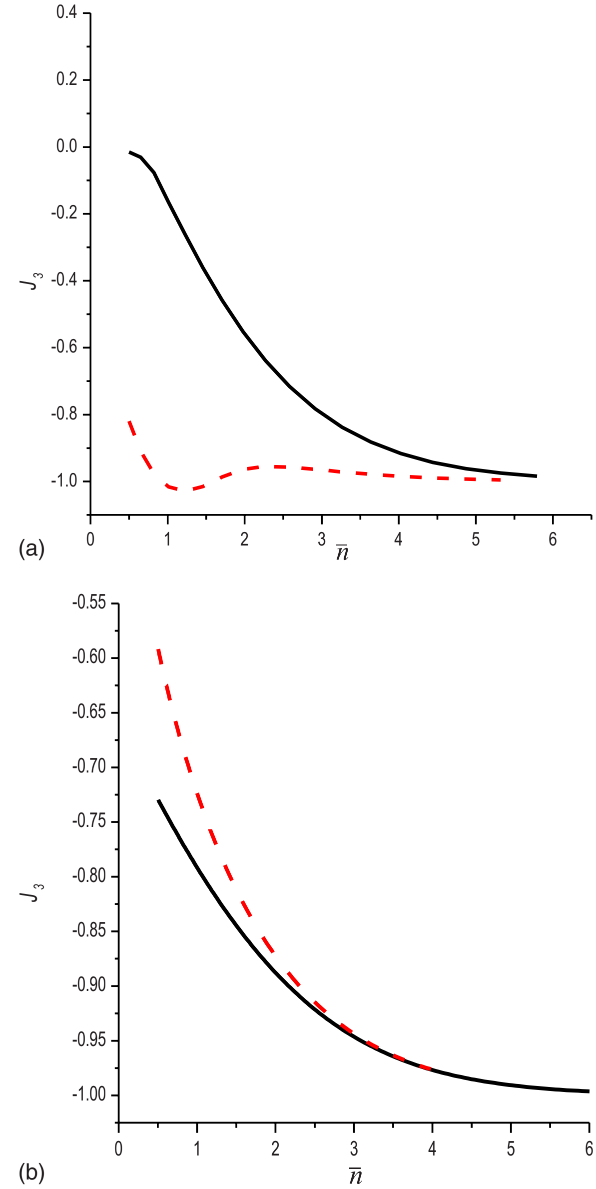

FIG. 8. (Color online) Extremal values of J_3 for (a) $\Phi=0$ and (b) $\Phi=\pi$.

$J_4=3.7$ for $\bar{n}=1$ and at the constant value $J_4=3$ for $\bar{n}\geq 3$, and for the latter J_4 rises up to the value $J_4=2$ for $\bar{n}\geq 3$. For $\Phi=\pi$ both cases, though different for low $\bar{n}$, J_4 goes asymptotically to $J_4=2$ for increasing $\bar{n}$. Thus, in all cases for large enough $\bar{n}$, we obtain violations of the inequality to a greater degree than seems possible with the *N*00*N* states.

V. CONCLUSIONS

In this paper, we have studied the violations of various Bell-type inequalities that can occur with maximally entangled coherent states and we have compared our results with those obtained by Wildfeuer *et al.* [5] for the so-called *N*00*N* states. We have found that, in many instances, the MECSs yield stronger violations of the various inequalities than is possible with the *N*00*N* states. The most dramatic example is with respect to the CHSH inequality which for the *N*00*N* states is violated only for case $N=1$, whereas for the MECS we obtain increasing violations approaching the Tsirelson bound with increasing average photon number $\bar{n}$. Interestingly, this result combines two aspects of the approach to quantum-optical interferometric metrology we have been advocating for some years: the use of MECS as opposed to *N*00*N* states, and the use of parity measurements on one of the output beams instead of coincidence counting as the latter becomes difficult if not impossible for large photon numbers. So far, *N*00*N* state experiments have been performed with two [22–26], three [27], four [28,29], and six [30] photons; but, as said in the introduction, the generation of a large *N* single-mode number state $|N\rangle$, which must then be transformed into a *N*00*N* state by a nonlinear interaction, would be very difficult. There is an inherent difficulty in generating *on demand* number states, especially for higher *N*. In contrast, coherent states of more or less arbitrary amplitudes are relatively easy to generate, though one would still

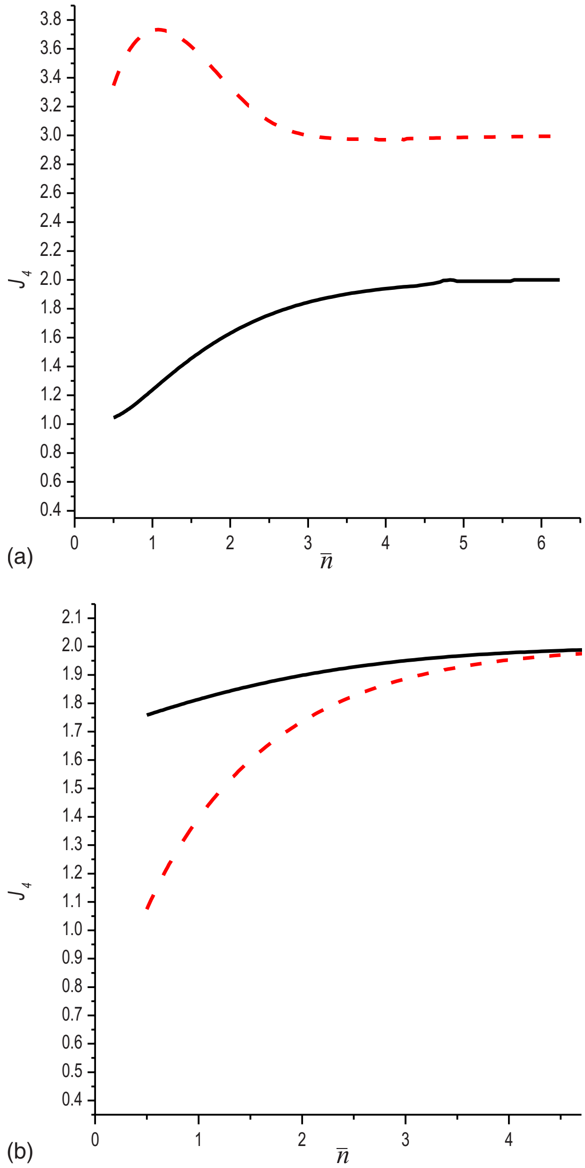

FIG. 9. (Color online) Extremal values of J_4 for (a) $\Phi=0$ and (b) $\Phi=\pi$.

need nonlinear interactions, as described in Refs. [11–13,17–19], to generate out of them the MECS, as described. Evidently, the results displayed in the present paper suggest that MECS would be of considerable advantage over the $N00N$ states for performing nonlocality tests on quantum mechanics versus local hidden-variable theories, particularly, for the violation of the parity-based CHSH inequality as discussed in Sec. III as these are violated to the highest degree possible, approaching the Tsirelson bound for large $\bar{n}$. Experimentally, it would be necessary to perform parity measurements on the field modes. Ideally, one could measure the photon number and raise -1 to that power; but that assumes the availability of photon detectors able to resolve counts at the level of a single photon. Progress has been made in that direction [31] though there is still the question of how high the photon numbers can be for those techniques to work. There is the possibility of performing quantum nondemolition (QND) measurements of parity directly without first measuring the photon number [32], but this requires a large cross-Kerr nonlinearity. However, a QND approach to measuring photon numbers using weak cross-Kerr nonlinearities has recently been discussed [33]. But some time ago, Wu [34] discussed the violation of the parity-based CHSH inequality for different types of two-mode states considered here and, in doing so, discussed the prospect of using homodyne detection which has high efficiency. Actually, he discussed two possibilities: optical homodyne tomographic detection and cascaded optical homodyne detection. In the former, the idea is to extend the procedure used to experimentally reconstruct the Wigner function of a single-mode field state [35] to a two-mode state. In the latter, one could extend the proposal of Kis *et al.* [36] to reconstruct a two-mode Wigner function by local sampling of the phase-space distribution. The proposal of [36] is based on any earlier work by Munroe *et al.* [37], which describes a method to resolve photon number distributions using balanced homodyne measurements. Detector inefficiencies in these schemes can be modeled via beam splitting (see Leonhardt in Ref. [35]). Finally, we note that the required displacement operation as performed with an unbalanced beam splitter was already been implemented experimentally by Lvovsky and Babichev [38].

ACKNOWLEDGMENTS

This research is supported by grants for the U.S. Department of the Army, Research Corporation, and PSC-CUNY.

APPENDIX

In this appendix, for the purpose of making comparison with our MECS results, we summarize and extend the Bell-type inequality results of Ref. [5] based on the $N00N$ states,

$$|\Psi_N\rangle = \frac{1}{\sqrt{2}}(|N\rangle_a|0\rangle_b + e^{i\varphi}|0\rangle_a|N\rangle_b). \qquad (37)$$

The authors of [5] considered only the case $\varphi=\pi$ throughout. We have considered also the case where $\varphi=0$. For the former case, we find some discrepancies with the results reported in [5].

In Fig. 10 we present the results for the CH inequality, where it is evident that identical results are obtained for both $\varphi=0$ and $\varphi=\pi$. The same is true for the CHSH inequality as can be seen in Fig. 11. Note that only for $N=1$ do we get a violation of the inequality, in agreement with Ref. [5]. For the quantities J_1 and J_2, we find total agreement with the results of [5] and can be seen in Figs. 12 and 13, though we add that the results are identical for both phases $\varphi=0$ and $\varphi=\pi$. For the quantities J_3 and J_4, given in Figs. 14 and 15, we have found some discrepancies. Our results for J_3 for $\varphi=0$ are identical to the results reported in [5] for the case $\varphi=\pi$, and our results for $\varphi=\pi$ are identical to those of [5], except for the case $N=1$, for which we obtain a much stronger violation of the inequality. Finally, for J_4 we are in agreement with Ref. [5] for all N except for the lowest cases where we find some small discrepancies.

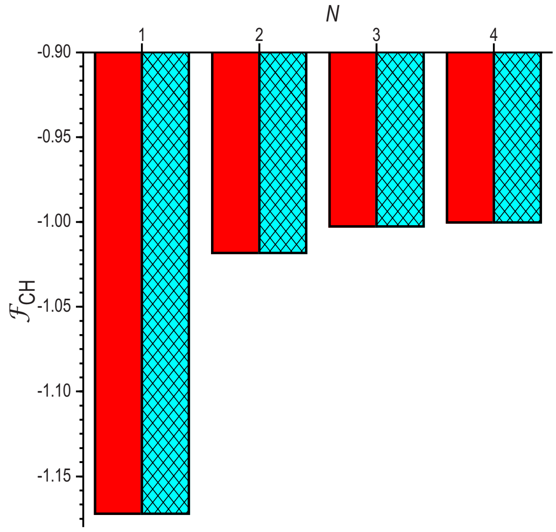

FIG. 10. (Color online) $\mathcal{F}_{\rm CH}$ versus N for the $N00N$ states with $\varphi=0$ on the right and $\varphi=\pi$ on the left.

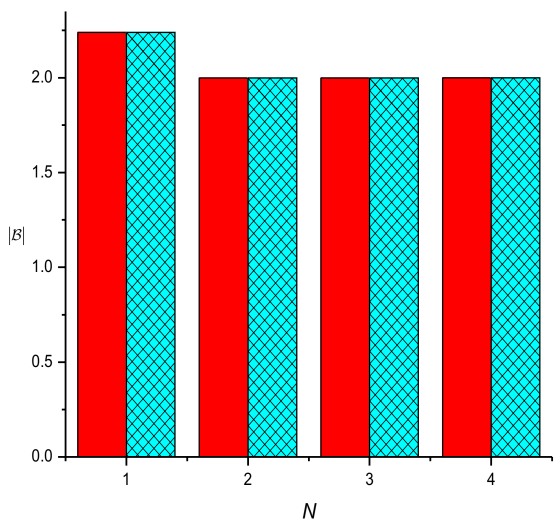

FIG. 11. (Color online) $|\mathcal{B}|$ versus N.

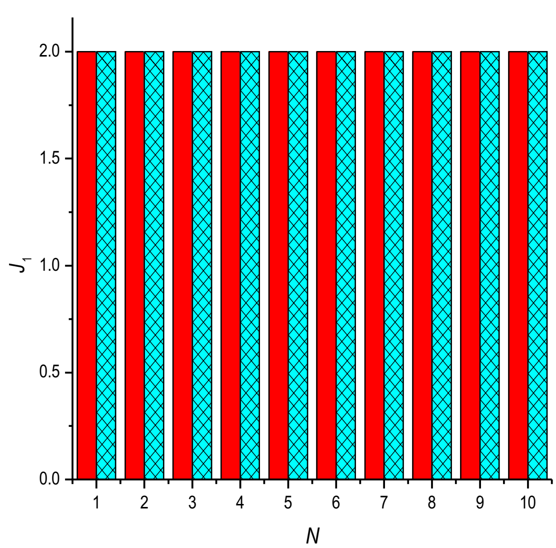

FIG. 12. (Color online) J_1 versus N.

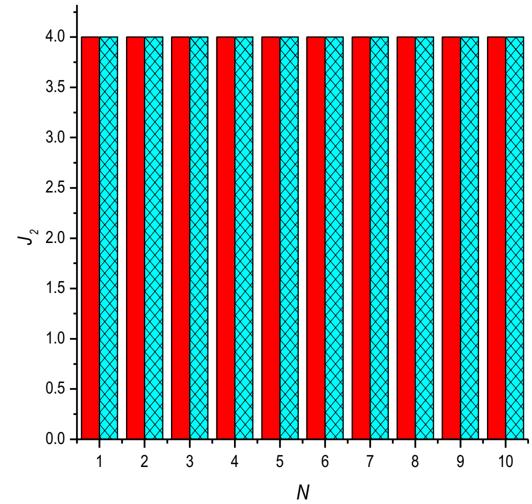

FIG. 13. (Color online) J_2 versus N.

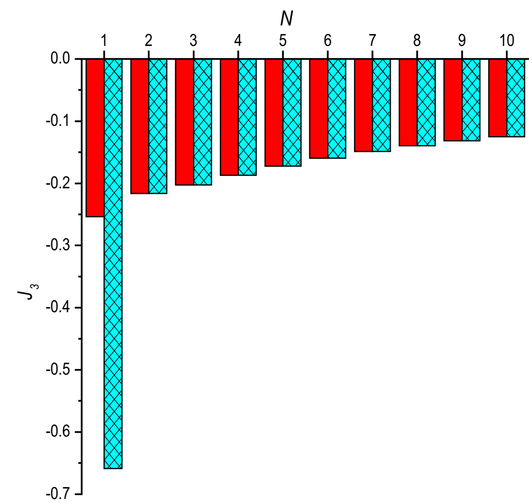

FIG. 14. (Color online) J_3 versus N. Note that our calculations for the case $N=1$ and $\varphi=\pi$ differ from those of Ref. [5] in that we obtain a much larger violation of the inequality, whereas their results for the same phase are identical to the ones we obtain for $\varphi=0$.

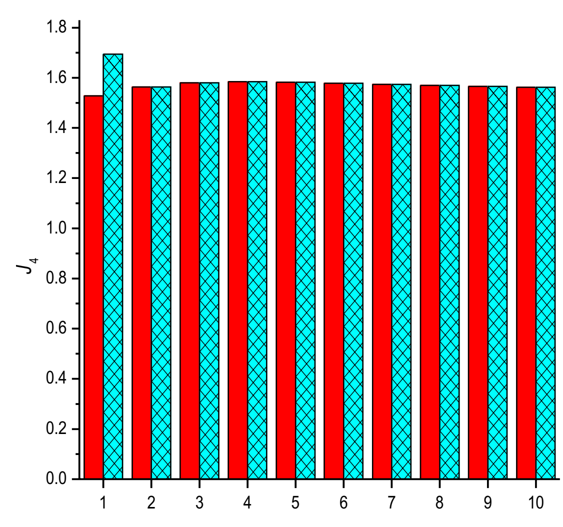

FIG. 15. (Color online) J_4 versus N. We obtain slightly different results than are reported in [5].

[1] For a recent review, see M. Genovese, Phys. Rep. **413**, 319 (2005).
[2] J. J. Bollinger, W. M. Itano, D. J. Wineland, and D. J. Heinzen, Phys. Rev. A **54**, R4649 (1996).
[3] See J. P. Dowling, Contemp. Phys. **49**, 125 (2008), and references therein.
[4] A. N. Boto, P. Kok, D. S. Abrams, S. L. Braunstein, C. P. Williams, and J. P. Dowling, Phys. Rev. Lett. **85**, 2733 (2000).
[5] C. F. Wildfeuer, A. P. Lund, and J. P. Dowling, Phys. Rev. A **76**, 052101 (2007).
[6] J. F. Clauser and M. A. Horne, Phys. Rev. D **10**, 526 (1974).
[7] J. S. Bell, Physics **1**, 195 (1964).
[8] S. Janssens, B. De Baets, and H. De Meyer, Fuzzy Sets Syst. **148**, 263 (2004).
[9] J. F. Clauser, M. A. Horne, A. Shimony, and R. A. Holt, Phys. Rev. Lett. **23**, 880 (1969).
[10] For the theory, see K. Banaszek and K. Wódkiewicz, Phys. Rev. Lett. **82**, 2009 (1999); the experiments are reported in S. A. Babichev, J. Appel, and A. I. Lvovsky, *ibid.* **92**, 193601 (2004); B. Hessmo, P. Usachev, H. Heydari, and G. Björk, *ibid.* **92**, 180401 (2004); M. D'Angelo, A. Zavatta, V. Parigi, and M. Bellini, Phys. Rev. A **74**, 052114 (2006).
[11] C. C. Gerry, Phys. Rev. A **61**, 043811 (2000); C. C. Gerry and A. Benmoussa, *ibid.* **65**, 033822 (2002).
[12] C. C. Gerry, A. Benmoussa, and R. A. Campos, Phys. Rev. A **66**, 013804 (2002).
[13] C. C. Gerry and R. A. Campos, Phys. Rev. A **64**, 063814 (2001).
[14] See M. Fleischhauer, A. Imamoglu, and J. P. Marangos, Rev. Mod. Phys. **77**, 633 (2005); A. André, M. D. Eisaman, R. L. Walsworth, A. S. Zibrov, and M. D. Lukin, J. Phys. B **38**, S589 (2005), for reviews and references therein; for a recent paper on the possible production of a giant cross-Kerr nonlinearity in a carbon nanotube, see H. Sun, X.-L. Feng, S. Gong, and C. H. Oh, Phys. Rev. B **79**, 193404 (2009).
[15] H. Lee, P. Kok, N. J. Cerf, and J. P. Dowling, Phys. Rev. A **65**, 030101(R) (2002).
[16] E. Knill, R. Laflamme, and G. J. Milburn, Nature (London) **409**, 46 (2001).
[17] C. C. Gerry, Phys. Rev. A **59**, 4095 (1999).
[18] H. Jeong, Phys. Rev. A **72**, 034305 (2005); B. He, M. Nadeem, and J. A. Bergou, *ibid.* **79**, 035802 (2009).
[19] S. Glancy and H. M. de Vasconcelos, J. Opt. Soc. Am. B **25**, 712 (2008).
[20] B. S. Cirel'son, Lett. Math. Phys. **4**, 93 (1980).
[21] I. Pitowsky, *Quantum Probability-Quantum Logic*, Lecture Notes in Physics Vol. 321 (Springer-Verlag, Berlin, 1989).
[22] C. K. Hong, Z. Y. Ou, and L. Mandel, Phys. Rev. Lett. **59**, 2044 (1987).
[23] J. G. Rarity, P. R. Tapster, E. Jakeman, T. Larchuk, R. A. Campos, M. C. Teich, and B. E. A. Saleh, Phys. Rev. Lett. **65**, 1348 (1990).
[24] A. Kuzmich and L. Mandel, Quantum Semiclassic. Opt. **10**, 493 (1998).
[25] E. J. S. Fonseca, C. H. Monken, and S. Pádua, Phys. Rev. Lett. **82**, 2868 (1999).
[26] K. Edamatsu, R. Shimizu, and T. Itoh, Phys. Rev. Lett. **89**, 213601 (2002).
[27] M. W. Mitchell, J. S. Lundeen, and A. M. Steinberg, Nature (London) **429**, 161 (2004).
[28] P. Walther, J.-W. Pan, M. Aspelmeyer, R. Ursin, S. Gaspraroni, and A. Zeilinger, Nature (London) **429**, 158 (2004).
[29] T. Nagata, R. Okamoto, J. L. O'Brien, K. Sasaka, and S. Takeuchi, Science **316**, 726 (2007).
[30] K. J. Resch, K. L. Pregnell, R. Prevedel, A. Gilchrist, G. J. Pryde, J. L. O'Brien, and A. G. White, Phys. Rev. Lett. **98**, 223601 (2007).
[31] See, for example, K. Banaszek and I. A. Walmsley, Opt. Lett. **28**, 52 (2003); M. J. Fitch, B. C. Jacobs, T. B. Pittman, and J. D. Franson, Phys. Rev. A **68**, 043814 (2003); D. Rosenberg, A. E. Lita, A. J. Miller, S. Nam, and R. E. Schwall, IEEE Trans. Appl. Supercond. **15**, 575 (2005).
[32] C. C. Gerry, A. Benmoussa, and R. A. Campos, Phys. Rev. A **72**, 053818 (2005).
[33] W. J. Munro, K. Nemoto, R. G. Beausoleil, and T. P. Spiller, Phys. Rev. A **71**, 033819 (2005); C. C. Gerry and T. Bui, Phys. Lett. A **372**, 7101 (2008).
[34] J. W. Wu, Phys. Rev. A **61**, 022111 (2000).
[35] For the theory, see U. Leonhardt, *Measuring the Quantum State of Light* (Cambridge University Press, Cambridge, 1997), and references therein; for experiments, see D. T. Smithey, M. Beck, M. G. Raymer, and A. Faridani, Phys. Rev. Lett. **70**, 1244 (1993); G. Breitenbach, S. Schiller, and J. Mlynek, Nature (London) **387**, 471 (1997); J. W. Wu, P. K. Lam, M. B. Gray, and H. A. Bachor, Opt. Express **3**, 154 (1998).
[36] Z. Kis, T. Kiss, J. Janszky, P. Adam, S. Wallentowitz, and W. Vogel, Phys. Rev. A **59**, R39 (1999).
[37] M. Munroe, D. Boggavarapu, M. E. Anderson, and M. G. Raymer, Phys. Rev. A **52**, R924 (1995).
[38] A. I. Lvovsky and S. A. Babichev, Phys. Rev. A **66**, 011801(R) (2002).